

# Synthesis and Characterization of Iron (III) Oxide Nanomaterials for Photocatalytic Degradation of Congo Red

Yonas Weldemariam<sup>1</sup>    Abi Tadesse<sup>2</sup>

1. Department of Chemistry, College of Natural & Computational Sciences, Aksum University, P.O Box 1010, Aksum, Ethiopia

2. Department of Chemistry, Haramaya University, P.O Box 138, Haramaya, Ethiopia

## Abstract

This paper reports the synthesis and characterization nano-sized Iron (III) oxide for photochemical degradation of reactive Congo red (CR). *The Fe<sub>2</sub>O<sub>3</sub> nanoparticles were prepared by simple aqueous combustion synthesis method using Fe(NO<sub>3</sub>)<sub>3</sub>·9H<sub>2</sub>O as an oxidant and N<sub>2</sub>H<sub>4</sub>CO as fuel at 1:1 ratio.* The synthesized photocatalysts were characterized by XRD, SEM, FTIR and Uv-vis Spectroscopy. The synthesized samples were tested as photocatalysts for the decomposition of Congo red dye under UV irradiation. The impact of crystal size, loading catalyst and irradiation time on the rate of decomposition of Congo red dye was investigated. The experimental results show that *CR degradation increased with increasing of crystal size, time and amount of loaded catalyst.*

**Keywords:** Characterization, Combustion Synthesis, Congo red, Photocatalysis, and UV irradiation.

## 1. INTRODUCTION

Organic dyes are essential dyes at textile, pharmaceutical, leather industries, but it is toxic pollutant when released to the environment as effluent, basically it affects water bodies, soil fertility and human health in general. They usually have synthetic origin & complex aromatic molecular structure which make them more stable & more difficult to be biodegraded.<sup>[1]</sup>

As international environmental standards are becoming more stringent, technological systems for the removal of organic pollutants, such as dyes have been recently developed. In recent years interest has been focused on the use of semiconductor materials as photocatalysts for the removal of organic from aqueous or gas phase. This is due to the fact that the process gradually breaks down the contaminant molecule, no residue of the original material remains and therefore no sludge requiring disposal to landfill is produced.<sup>[2-3]</sup>

Additionally, because the contaminant is attracted strongly to the surface of the catalyst, the process will continue to work at very low concentrations allowing sub part-per-million contents to be achieved. Taken together, these advantages mean that the process results in considerable savings in the water production cost and keeping the environment clean.<sup>[4-5]</sup>

In this regard, Iron oxide assisted photocatalysis and photo oxidation of organic contaminants was found to be highly effective, environmental compatibility, low cost and less complicated techniques for converting pollutants into relatively harmless byproducts.<sup>[6-8]</sup> In this paper, we report synthesis and characterization of Iron (III) oxide nanopowder for photodegradation of Congo red under UV irradiation.

## 2. MATERIALS & METHODS

### 2.1 Experimental Procedures

40.4g Fe(NO<sub>3</sub>)<sub>3</sub>·9H<sub>2</sub>O was dissolved in 25 mL distilled water and 6.06 g Urea was also dissolved in 10 mL distilled water with continuous stirring. Then, the solution of Fe(NO<sub>3</sub>)<sub>3</sub>·9H<sub>2</sub>O was added to the Urea solution under vigorous stirring. After mixing a brown gel was appeared. To this; 5ml of distilled water was added. After being stirred for 30 min, a transparent solution was observed and then the solution was transferred into evaporating dish and dried in an oven at 120 °C for 5 hrs. After drying, cooling and milling, it annealed at (400, 600, 800, and 1000 °C). Finally, the annealed sample was cooled and kept for further analysis.

The prepared samples were characterized using XRD, SEM, FTIR and UV-vis techniques. The crystallinity and phase identification were determined by powder XRD using Cu K $\alpha$  radiation ( $\lambda=0.15405$  nm) at the range of 4<sup>o</sup>-64<sup>o</sup>. SEM analysis was recorded with a Jeol (model JSM-5800) instrument after coating the samples with gold. The obtained micrograph of the synthesized Fe<sub>2</sub>O<sub>3</sub> is shown in Fig 2 a & b. For FTIR studies a small amount of nanoparticles were milled with KBr and then pressed into a disc for FTIR (IR Prestige-21, FTIR-8400S) analysis in the range of 4000-500 cm<sup>-1</sup>. In our work, we used UV-vis spectrophotometer (GALLENKAMP, UK, Sanyo SP-65) to estimate the band gap energy of the synthesized photocatalysts, and the spectra were measured in the range of 300-1100 nm.

For most photocatalysis measurement, the reaction suspension was prepared by adding 50 mg catalyst into 100 mL of CR solution (15 mgL<sup>-1</sup>), then magnetically stirred in the dark for 30 min then, the reactor bottle was exposed to the UV lamp 365 nm for 180 min at room temperature. <sup>[9]</sup> At every 20 min 10 mL of the samples was withdrawn from the reaction system, centrifuged and filtered. Then, the filtrate was determined by the light absorption at 500 nm using a UV-Vis.

### 3. RESULTS AND DISCUSSION

#### 3.1. Synthesis of Photocatalysts

It is observed that the color intensity was varied with calcinations temperature. Samples calcinated at 400 °C showed dark red color and as the temperature rose to 600, 800 and 1000 °C they changed to red color showing phase change from maghemite ( $\gamma$ -Fe<sub>2</sub>O<sub>3</sub>) to hematite ( $\alpha$ -Fe<sub>2</sub>O<sub>3</sub>) which is consistent with the reported observation.<sup>[9-10]</sup>

#### 3.2. Characterization of Catalysts

Selected series Fe<sub>2</sub>O<sub>3</sub> samples were examined by XRD. Fig. 1. shows the XRD patterns of nano sized Fe<sub>2</sub>O<sub>3</sub> prepared at 800 °C for 2 hour. The diffraction peaks, centered at  $2\theta \approx 24.3(012)$ ,  $33.2(104)$ ,  $35.7(110)$ ,  $40.80(113)$ ,  $49.55(024)$ , and  $54.25(116)$  assigned to  $\alpha$ -Fe<sub>2</sub>O<sub>3</sub> phase with rhombohedral structure and this matches well with the reported data on hematite iron oxide.<sup>[11-13]</sup> This confirms that the combustion synthesized samples were predominantly  $\alpha$ -Fe<sub>2</sub>O<sub>3</sub> phase. In case of sample annealed at 400 or 600 °C, the  $35.7^\circ$  peak could be due to either alpha or gamma phases. The mixed color of samples, the black due to ( $\gamma$ -Fe<sub>2</sub>O<sub>3</sub>) and red ( $\alpha$ -Fe<sub>2</sub>O<sub>3</sub>) also confirmed this fact. As the increase of sintering temperature enhances crystal transformation of Iron(III) oxides from maghemite to hematite, at temperature > 600 °C all the maghemite were converted to final product phase i.e. hematite and hence at this temperature the peak at  $35.7^\circ$  belongs to hematite.<sup>[14]</sup>

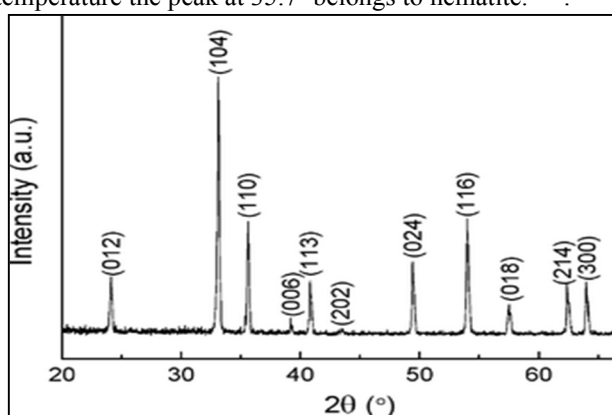


Fig.1. XRD patterns of Fe<sub>2</sub>O<sub>3</sub> sintered at 800 °C.

It has been reported that the variation of the annealing temperature can lead to an increase or decrease of the size of the particles depending on the concentration of the reactants and the particular route chosen for the preparation.<sup>[14-15]</sup> In our case, samples prepared at 400, 600, 800 and 1000 °C the average crystal size of Fe<sub>2</sub>O<sub>3</sub> which was calculated from the full width at half maximum of the peak (FWHM) by using Debye-Scherrer formula were found to be 28.17, 34.04, 37.88, and 43.96, respectively.

From the result, as the annealing temperature increases from 400 to 1000°C the crystal size increase from 28.17 to 43.96 nm. This shows that increasing the annealing temperature results in Fe<sub>2</sub>O<sub>3</sub> crystals with higher crystallite size and lower widths of the diffraction peak, which confirms the possibility of producing better quality crystals at higher annealing temperatures.

From UV-vis DRS, it is confirmed that the optical property of samples also varied with the variation of annealing temperature. To see the effect, the optical spectra of S<sub>A</sub>, S<sub>B</sub>, S<sub>C</sub> and S<sub>D</sub> were measured in UV-vis region. The result shows that the absorbance is well extended to the visible region as the annealing temperature increased. This is because of increasing annealing temperature increases crystallite size which in turn results a decrease in band-gap energy. Therefore, the absorption band shifts toward the longer wavelength region. This phenomenon could be explained by the quantum size effect of semiconductors. In the quantum size effect, the band-gap energy decreases as the crystallite size increases.<sup>[16]</sup>

SEM micrograph of as synthesized Fe<sub>2</sub>O<sub>3</sub> is shown in Fig. 2 a & b. In our case, SEM was used to study the morphological features and surface characteristics of photocatalyst material. Photographs show surface structure and porosity of Fe<sub>2</sub>O<sub>3</sub> particles. It also shows small spherical particles of nearly equal size (Fig. 2a).

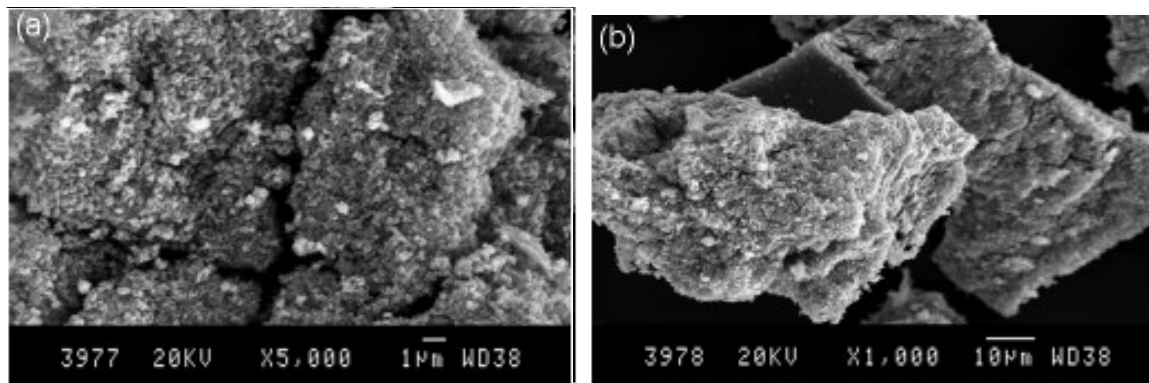


Fig 2. SEM image of as synthesized powder  $Fe_2O_3$  at magnification (a)  $1 \mu m$ , and (b)  $10 \mu m$

In case of FTIR studies, since the most promising region for studying the IR spectra of Iron(III) oxide is the mid-infrared,<sup>[16-17]</sup> the analysis have done in the range of  $4000-500 \text{ cm}^{-1}$ . In result, we observe various peaks showing the main absorption bands and other peaks resulted from surface adsorbed molecules. For all catalysts, the broad peaks in the range of  $3318-3450 \text{ cm}^{-1}$  and the narrow peak at about  $1615 \text{ cm}^{-1}$  are attributable to the O–H stretching and bending vibration of water and an OH group adsorbed on the surface of iron oxides.<sup>[17]</sup> In the low frequency region of FTIR spectra, a medium peak appeared at  $554 \text{ cm}^{-1}$  which is indicative peak of the Fe–O stretching vibration in iron oxide for  $Fe_2O_3$  and some other peaks at  $560, 655, \text{ and } 696 \text{ cm}^{-1}$  are also attributable to the Fe–O vibration. This agreed with previous literature report on<sup>[18-19]</sup> and supports the result obtained by XRD.

### 3.3 Photodegradation of Congo red

Under UV irradiation, the degradation of CR without the prepared catalyst at 180 min was 0.73%. This shows that CR is almost none degradable under this irradiation when there is no catalyst in the reaction system. Further, the percentage degradation of CR, without irradiation on the adsorbents ( $S_A, S_B, S_C$  and  $S_D$ ) was found to be 2.9, 3.4, 4.3 and 5.2, respectively.

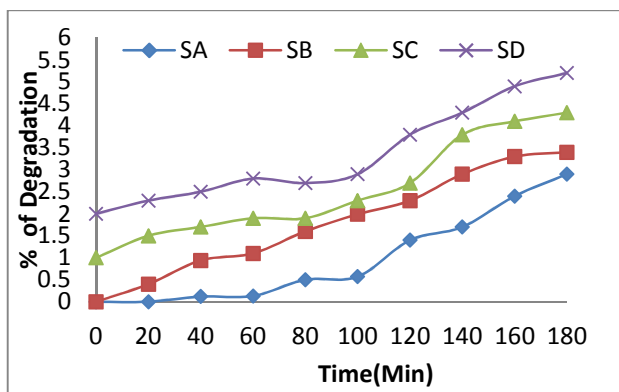


Fig.3. Degradation of CR over different catalysts without UV light irradiation

#### A. Effects of irradiation time

To study the effect of irradiation time 50 mg of each catalyst were tested. In this experiment, the extent of degradation was measure at 20 min interval. With increasing degradation time, the % of degradation increased.

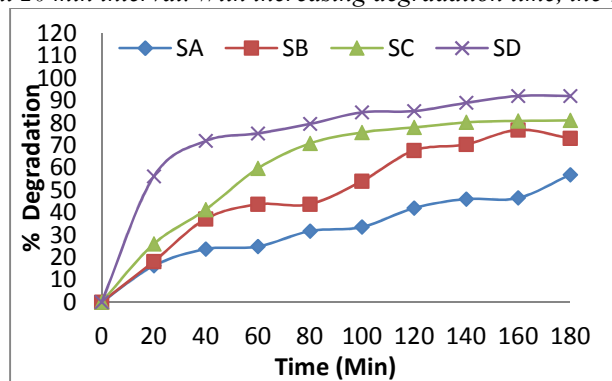


Fig 4. The extent of degradation of CR as a function of irradiation time.

The maximum degradation over  $S_A, S_B, S_C$  and  $S_D$  obtained after 3 hours irradiation was 56.88, 73.18, 81.16 and

92.14 %, respectively. This assured that all the synthesized catalysts are effective for degradation of CR dye under UV illumination.

### B. Effects of Crystal size

Here, we compared four catalysts sintered at different temperatures. The percentage degradation of CR slightly increased with increasing crystal size. At the end of 180 minutes, 56.88, 74.18, 81.16 and 92.14 percent of CR was degraded on the surface of S<sub>A</sub>, S<sub>B</sub>, S<sub>C</sub> and S<sub>D</sub>, respectively.

It is well-observed that the crystallinity plays an important role in improving the photocatalytic activities of hematite and is more important than other factors.<sup>[5, 16]</sup> From the decolorization data of CR in Fig. 5, the Iron(III) oxide with 28.17 nm crystal size has the lowest catalytic activity and the activity increased in the order of 28.17 < 34.04 < 37.88 < 43.96 nm. The catalytic performance enhancement may be mainly due to the improvement in crystallinity of the hematite nanoparticles.

### C. Effects of loading catalyst

In this case, we carried out by taking different amounts of Fe<sub>2</sub>O<sub>3</sub> and keeping CR at 15 mg L<sup>-1</sup>.

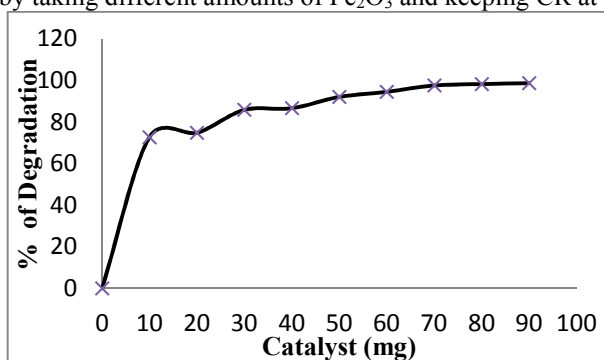


Fig 5. The effect of amount of catalyst on photocatalytic degradation of CR.

As we can see from figure 5., It is found that the increase in the catalyst amount increases the degradation of CR; this could be due to an increase in active sites available on the catalyst surface for the reaction, which, in turn, increases the rate of radical formation.<sup>[13, 16]</sup>

## 4. CONCLUSION

It is noted that in contrast to some other methods it is simple and convenient to prepare desired nanosized Fe<sub>2</sub>O<sub>3</sub> catalysts. It was observed that a variation in the annealing temperature in the range 400 to 1000°C is able to produce large size variation and slight change in the color of the samples. Hence, it was concluded that the increasing of calcinations temperature increases crystallite size and decreases the band gap energy hence, the absorbance of catalysts extended to visible light region. That is why excessive percentage of CR was degraded over catalysts having large crystallite size.

Over all, it was concluded that increasing crystal size, loaded catalyst and irradiation time increases percentage degradation, and combustion synthesized Fe<sub>2</sub>O<sub>3</sub> is powerful to degrade the CR organic dye, almost completely.

## ACKNOWLEDGMENTS

First, we would like to present our special thanks to Arba Minch University (AMU) for their financial support. We also thank to Department of Chemistry and, Department of Environmental & Water Supply Engineering (AMU) for their special cooperation and willingness to use their laboratory with its full equipment.

## REFERENCES

1. K. Honda, A. Fujishima, Nature 238 (1972) 37.
2. K. Sayama, R. Abe, H. Arakawa, H. Sugihara, Catal. Comm. 7 (2006) 96.
3. S.U.M. Khan, J. Akikusa, Journal of Phys. Chem. B 103 (1999) 7184.
4. Q. Ahsanulhaq, J.H. Kim, Y.B. Hahn, Nanotechnology 18 (2007) 485307.
5. R. Skomski, Journal of Phys.: Condens. Matter. 15 (2003) R841.
6. M.H. Khedr, K.S. Abdel Halimb,, N.K. Soliman, Synthesis and photocatalytic activity of nano-sized iron oxides, Materials Letters 63 (2009) 598–601.
7. Duhan. S, D.S, Synthesis and Structural Characterization of Iron Oxide-silica Nanocomposites Prepared by the Solgel Method, International Journal of Electronics Engineering, 2(1), 2010, pp. 89-92.
8. Miyata, T., Ishino, Y., and Hirashima T., 1978. Catalytic reduction of aromatic nitro compounds with hydrazine hydrate in the presence of Iron(III) oxide hydroxide. Synthesis pp. 834-835.
9. V.K. Jones, L.R. Neubauer, C.H. Bartholomew, J. Phys. Chem. 90 (1986) 4832.

10. X. Teng, H. Yang, *Journal of Mater. Chem.* 14 (2004) 774.
11. Fox, M.A., Dulay, M.T., (1993), Heterogeneous photocatalysis. *Chemical Reviews* 93:341-357.
12. B. Zhao, y. Wang, h. Guo, j. Wang, y. He, z. Jiao, m. Wu, Iron oxide(III) nanoparticles fabricated by electron beam irradiation method, *Materials Science-Poland*, Vol. 25, No. 4, 2007.
13. F.B. Li, X.Z. Li, C.S. Liu, Effect of alumina on photocatalytic activity of iron oxides for bisphenol A degradation, *Journal of Hazardous Materials* 149 (2007) 199–207.
14. Cornell, R.M. and Schwertmann, U. *The Iron Oxides. Structure, Properties, Reactions and Uses*; VCH Weinheim, 1996.
15. Silber S., Reuter E., Stuttgen A., and Albrecht G., 2002. (In Chinese). *Prog. Org. Coat.* Vol.45, pp. 259-256.
16. Cudennec, Y.; Lecerf, A. *Solid State Sci.* 2005, 7, 520–529.
17. Arslan I. *Journal of Hazard Mater Bul* 2001; 85:229.
18. M.A. Karakassides, D. Gournis, A.B. Bourlinos, P.N. Trikalitis, T. Bakas, Magnetic Fe<sub>2</sub>O<sub>3</sub>–Al<sub>2</sub>O<sub>3</sub> composites prepared by a modified wet impregnation method, *J. Mater. Chem.* 13 (2003) 871–876.
19. Houas A, Bakir I, Ksibi M, Elaloui E. *J Chim Phys* 1999; 96:479.